Fluctuation measurements in tokamaks with microwave imaging reflectometry[a)]

E. Mazzucato,[b)] T. Munsat, and H. Park
Princeton Plasma Physics Laboratory, Princeton, New Jersey 08543

B. H. Deng, C. W. Domier, and N. C. Luhmann, Jr.
Department of Applied Sciences, University of California at Davis, Davis, California 95616

A. J. H. Donné and M. J. van de Pol
FOM-Instituut voor Plasmafysica Rijnhuizen, Associatie EURATOM-FOM, P.O. Box 1207, 3430 BE Nieuwegein, The Netherlands

(Received 25 October 2001; accepted 16 November 2001)

To study the mechanism of anomalous transport in tokamaks requires the use of sophisticated diagnostic tools for the measurement of short-scale turbulent fluctuations. In this article, we describe an attempt at developing a technique capable of providing a comprehensive description of plasma fluctuations with $k_\perp \rho_i < 1$, such as those driven by the ion temperature gradient mode in tokamaks. The proposed method is based on microwave reflectometry, and stems from a series of numerical calculations showing that the spatial structure of fluctuations near the cutoff could be obtained from the phase of reflected waves when these are collected with a wide aperture optical system forming an image of the cutoff onto an array of phase sensitive detectors. Preliminary measurements with a prototype apparatus on the Torus Experiment for Technology Oriented Research 94 (TEXTOR-94) [U. Samm, *Proceedings of the 16th IEEE Symposium on Fusion Engineering, 1995* (IEEE, Piscataway, NJ, 1995), p. 470] confirm the validity of these conclusions. Technical issues in the application of the proposed technique to tokamaks are discussed in this article, and the conceptual design of an imaging reflectometer for the visualization of turbulent fluctuations in the National Spherical Torus Experiment (NSTX) [M. Ono *et al.*, Nucl. Fusion **40**, 557 (2000)] is described.
 [DOI: 10.1063/1.1435564]

I. INTRODUCTION

Understanding the mechanism of anomalous transport in tokamaks is one of the great challenges of fusion research. Indeed, since most explanations of this phenomenon are based on some type of turbulence,[1,2] understanding anomalous transport is tantamount to understanding plasma turbulence.

In tokamak research, a longstanding conjecture is that the observed anomalous plasma transport is caused by some type of drift wave instability. Accordingly, for turbulent fluctuations that are isotropic perpendicularly to the magnetic field, the energy replacement time (τ_E) must exhibit a Bohm scaling [$\tau_E \propto \Omega^{-1}(a/\rho_i)^2$] when $k_\perp \propto a^{-1}$, and a Gyro-Bohm scaling [$\tau_E \propto \Omega^{-1}(a/\rho_i)^3$] when $k_\perp \propto \rho_i^{-1}$ (here and in the following, a is the plasma minor radius, $k_\perp$ is the fluctuation wave number perpendicular to the magnetic field, Ω is the ion cyclotron frequency and ρ_i is the ion Larmor radius). For anisotropic turbulence, predictions become more complex. For instance, τ_E can follow a Gyro-Bohm scaling for $k_\theta \propto a^{-1}$ and $k_r \propto (a\rho_i)^{-1/2}$ (where k_θ and k_r are the poloidal and radial components of $k_\perp$, respectively).

Empirical scalings of τ_E tend to support a Gyro-Bohm scaling, even though they all contain other dimensionless parameters besides the normalized Larmor radius ρ^* $(=\rho_i/a)$. A case in point is that used to predict the performance of the International Thermonuclear Experimental Reactor,[3] which in standard notation is $\tau_E \Omega \propto \rho^{*-2.70}\beta^{-0.90}\nu^{*-0.01}M^{0.96}q_{95}^{-3.0}A^{-0.73}\kappa^{2.3}$. Unfortunately, such empirical scalings find meager support in the existing data base of turbulence measurements.

The main difficulty in drawing any firm conclusion from fluctuation measurements is their scarcity and limitations. For example, wave scattering measurements,[4–8] which were so prominent in early fluctuation studies, have a poor spatial resolution—in most cases larger than the plasma minor radius. The method of beam emission spectroscopy[9] needs a perturbing neutral beam and has serious difficulties in detecting plasma fluctuations in the central core of large tokamaks. The interpretation of microwave reflectometry is very difficult, and in the best of cases it cannot be done unambiguously.[10–12] The inevitable conclusion is that, for advancing our understanding of turbulence, we must improve the capability of our diagnostic tools.

In this article, we describe a novel technique for the global visualization of short-scale fluctuations with $k_\perp \rho_i < 1$ in the main core of tokamak plasmas. The outline is as follows. In Sec. II, the intrinsic difficulties and limitations in the use of standard reflectometry in tokamaks are discussed and explained using the results of a series of numerical simulations. The method of microwave imaging reflectometry is

[a)]Paper RI2 4, Bull. Am. Phys. Soc. **46**, 289 (2001).
[b)]Invited speaker. Electronic mail: mazzucato@pppl.gov

spectrum of probing wave numbers.[13] To perform this function, the optical system must have two different focal points, one located at the center of the torus in the equatorial plane, the second at the center of curvature of the cutoff surface in the poloidal plane. It should also be noted that without this curvature matching, any small deviation in the radial position of the cutoff would cause large deviation of the reflected beam, and degradation of the spectrum of collected radiation. By using the curvature-matching technique, cutoff surfaces over a wide range of densities can be illuminated with minimal changes to the illumination optics.

For the reflected wave, the function of the optical system is that of creating an image of the virtual cutoff onto an array of detectors. This is illustrated in Fig. 6(b), which shows the reflected beam from three points of the virtual cutoff (located behind the actual cutoff as described in Sec. II). To overcome the limitation on the amount of power available for the probing beam, it may be convenient to use additional optics (not shown in Fig. 6) for demagnifying the image as much as possible consistently with the detector element size. Furthermore, additional optics may also be needed to compensate for the two different focal points of the primary optics.

In a realistic diagnostic configuration, the main optical illumination will be imposed by the size of the vacuum window. Assuming that the rest of the optical system does not vignette the reflected beam, and a Gaussian radiation profile for the detectors, the best instruments resolution will be given by the Gaussian "spot-size" at the cutoff, given by $2\delta = 2\lambda d/\pi r$ (where δ is the Gaussian beam waist at the object plane, λ is the wavelength of the probing beam, d is the distance from the aperture to the beam waist, and r is the window radius). Clearly it is possible for the instrument resolution to be different in the toroidal and poloidal directions. Furthermore, the resolution of off-axis channels could be degraded by further vignetting of the reflected signal.

The amount of coverage in the plasma, which also determines the lower limit of the k_θ resolution, will also be constrained by the window size. This is obvious from Fig. 6(a), which shows how the size and location of the window relative to the cutoff surface determine the illuminated plasma region. A further limitation is that, for avoiding diffraction from the window edge, the beam profile must fall off near the window edges.

The viability of imaging reflectometry is dependent on the availability of sensitive detectors. In this regard there has been steady progress in the area of millimeter-wave detectors, particularly in the design of arrays that could be inexpensively manufactured on printed circuit boards, and therefore could scale-up to large multichannel arrays.[16]

Figure 7 illustrates the conceptual design of a microwave imaging reflectometer for the National Spherical Torus Experiment (NSTX), a low aspect ratio tokamak with the mission of investigating the physics of high beta plasmas.[17] Some of its parameters are major radius 0.85 m, minor radius 0.67 m, toroidal magnetic field 0.3–0.45 T, plasma current 0.7–1.4 MA, and central temperatures 0.5–2.0 keV.

Compared to the scheme of Fig. 6, the major innovation in the design of Fig. 7 is the use of reflective optics for avoiding the spurious effects of internal reflections in refractive optics. Figure 7(a) shows the ray trajectories (dashed lines) of a 65 GHz probing beam (X-mode) together with the trajectories (solid lines) of the reflected wave in the absence of plasma fluctuations. The coincidence of these two sets of trajectories demonstrates a nearly perfect matching of the probing wave front to the cutoff curvature. Figure 7(b) shows the ray trajectories of six backward waves that are born on the equatorial plane (near the cutoff) with a wave number $\leqslant 2.0\ \mathrm{cm}^{-1}$ (to be compared with $0.5\ \mathrm{cm}^{-1}$ for the poloidal wave number of expected fluctuations in NSTX plasmas). These waves are focused on a single point of the detector plane—the image of the virtual cutoff. The position of the latter is indicated in Fig. 7(b) by the intersection of the dashed lines. The illuminated plasma area is ~25 cm tall, resulting in a lower limit of $0.25\ \mathrm{cm}^{-1}$ for the wave number resolution. Finally, the spatial resolution in the poloidal direction is ~0.5 cm.

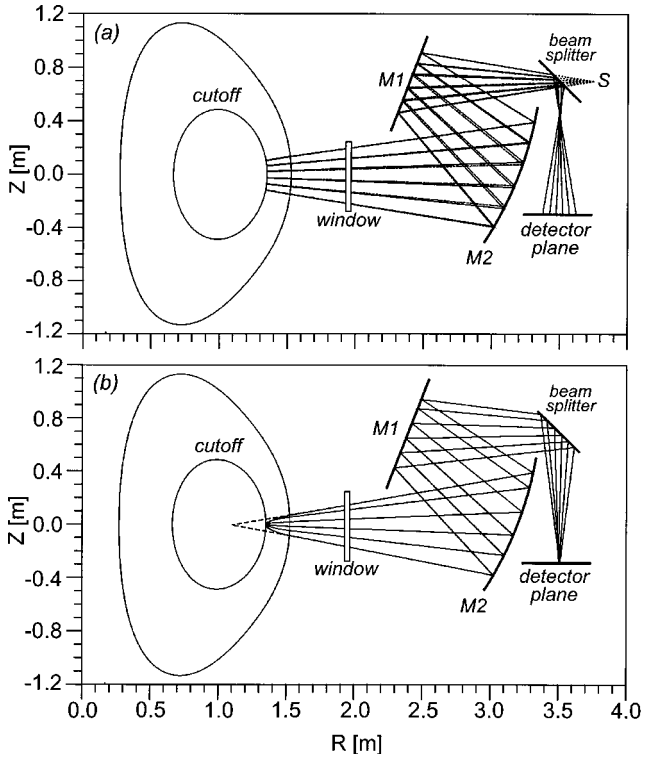

FIG. 7. Conceptual design of an imaging reflectometer for NSTX; S is the microwave source, M1 and M2 are cylindrical mirrors. Ray trajectories are from a ray tracing code including plasma refraction.

IV. PRELIMINARY RESULTS

Recently, the first experimental application of imaging reflectometry to tokamaks has been made on TEXTOR-94[18] (Torus Experiment for Technology Oriented Research 94) a circular cross section tokamak with $a=0.50$ m, $R=1.75$ m, and $B\leqslant 2.9$ T. The reflectometer was built using the optical components of an electron cyclotron emission (ECE) imaging apparatus, which was used previously for the study of temperature fluctuations in TEXTOR-94.[19,20] Indeed, this underscores one of the main advantages of imaging reflectometry, i.e., the possibility of sharing the optics with an ECE imaging system, and thus making possible a tool for the si-

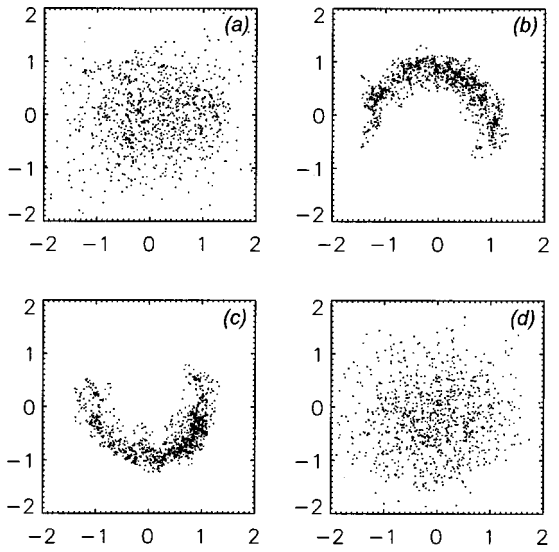

FIG. 8. Quadrature signals plots (normalized to unit average power) over a 3 ms time window as the cutoff moves through the optical focal plane because of a density rise. Cutoff positions are 1.93 m (a), 1.99 m (b) and (c), and 2.06 m (d).

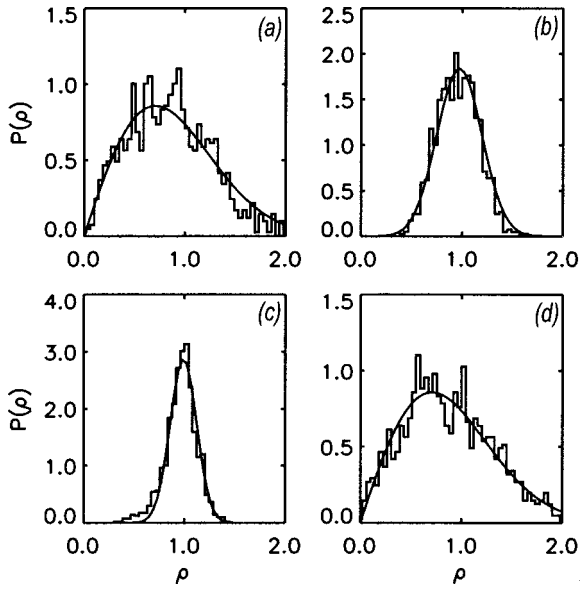

FIG. 9. Amplitude histograms of the signals of Fig. 9 and best fit to a Rice distribution (smooth lines). The Rice parameters $[\rho_0, \sigma]$ are [0.00, 0.71] (a), [0.95, 0.22] (b), [0.98, 0.14], (c), and [0.00, 0.71] (d).

multaneous visualization of both density and temperature fluctuations. The development of such a system is the goal of an ongoing collaboration between the University of California at Davis, the Princeton Plasma Physics Laboratory and the FOM Institute for Plasma Physics.

The prototype imaging reflectometer, whose scheme was basically that shown in Fig. 6, shared the vacuum window with the Thomson scattering apparatus. In this experiment, both the probing frequency (84 GHz, X-mode) and the focal plane of the optics were held fixed, and the electron density was ramped during the shot to bring the cutoff surface through and beyond the focal plane of the optics. Figure 8 shows some *I/Q* plots from a single channel recorded over several 3 ms time windows as the central plasma density changed from 2.8×10^{19} m^{-3} at $t=1.2$ s [Fig. 8(a)], to 4.4×10^{19} m^{-3} at $t=2.4$ s [Fig. 8(d)]. During the density ramp, the cutoff position moved from 1.93 to 2.06 m [with an intermediate position of 1.99 m at the time of both plots (b) and (c)].

The striking difference between plots (a,d) and (b,c) is in the level of amplitude fluctuations, which is much larger in the former case. These data were collected in ohmic plasmas where, apart from a small density rise, all plasma parameters were stationary. Thus, consistent with the numerical results of Fig. 3, we attribute the much smaller level of amplitude fluctuations of plots (b,c) to the in-focus condition of the virtual cutoff. This is confirmed by the agreement between the numerical estimate of its position in plots (b,c) with the radial position of the focal plane, and by the fact that the distance between the cutoffs of (a) and (b) or between those of (c) and (d) is larger than the optical depth of focus.

The histograms of the signal amplitude are displayed in Fig. 9 together with the best fit to the Rice probability distribution [Eq. (3)]. This shows that the amplitude of the coherent reflection goes from zero during out-of-focus conditions to close to unity when the virtual cutoff is in-focus. The fact that the Rice distribution appears to describe the distribution of amplitudes even during the in-focus conditions can be explained by a residual of amplitude fluctuations, as shown by the numerical simulations [Fig. 3(b)], and by a nonperfect focusing of the cutoff because of optical aberrations.

Another remarkable difference between the in-focus and the out-of-focus conditions is the time evolution of the phase of measured signals. This is illustrated in Fig. 10, which shows that during out-of-focus conditions the average rate of change is more than two orders of magnitude larger than during in-focus conditions. This phenomenon, which cannot be explained with the rise in density, is known in standard

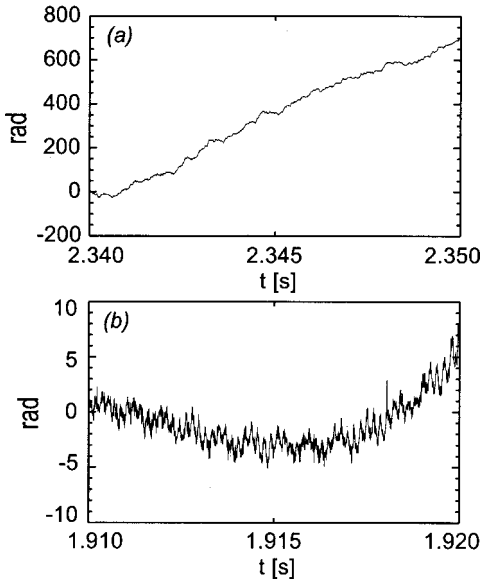

FIG. 10. Time evolution of the signal phase during out-of-focus (a) and in-focus (b) cutoff positions.

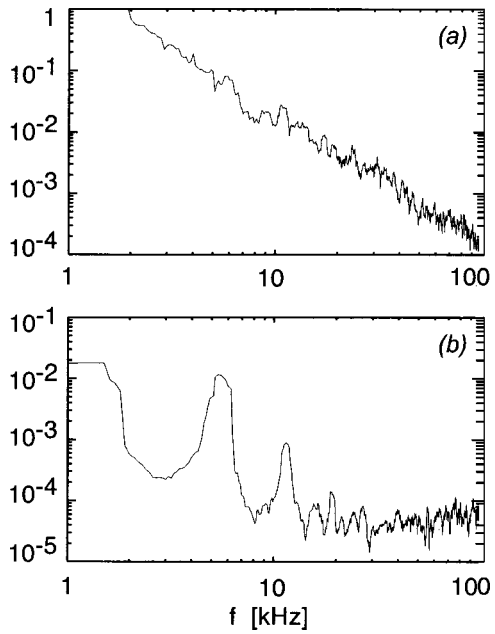

FIG. 11. Power spectrum of the signal phase for out-of-focus (a) and in-focus (b) cutoff positions.

reflectometry as the *runaway-phase* phenomenon. Similarly, the power spectra are also very different in the two cases, as illustrated by Fig. 11 where the phase power spectrum is dominated by large coherent MHD fluctuations when the cutoff is the in-focus, while it becomes a featureless $1/f^2$ spectrum when the cutoff goes out-of-focus. What is remarkable is that in the latter case, the spectrum does not give the slightest hint of the presence of large MHD fluctuations. Again, this is a known phenomenon in standard reflectometry,[12] whose cause has always been a matter of conjecture. This effect appears to be fully explained by our measurements.

These measurements confirm the validity of our numerical results (Sec. II) that are at the basis of microwave imaging reflectometry, and clearly demonstrate the advantages of this technique over standard reflectometry—regardless of whether the measurement is a single or a multi-point measurement. The fact that the introduction of focusing optics allows multiple channels measurements must be considered just a fringe benefit of the proposed method.

V. CONCLUSION

In summary, our numerical results support the conjecture that the chaotic behavior of signals in standard reflectometry is due to the interference of reflected waves at the point of measurement. This is caused by the scattering of reflected waves over a large angle by the 2D structure of tokamak fluctuations. The numerical results suggest that a mapping of fluctuations near the cutoff could be obtained from the phase of measured signals if the reflected waves are collected with a wide aperture antenna, and an image of the cutoff is made onto an array of microwave detectors (taking plasma refraction into account). These conclusions appear to be fully confirmed by measurements on TEXTOR-94 using a prototype imaging reflectometer.

These results form the bases of an apparatus—currently under construction—that will be used on TEXTOR-94 for the study of turbulent fluctuations in plasmas with a dynamic ergodic divertor. The reflectometer will operate in the frequency range 84–90 GHz using the optical scheme of Fig. 7, which will be shared with an electron cyclotron imaging system[20] operating in the frequency range 110–140 GHz. A dichroic plate will be used to separate the reflectometer signal from the plasma cyclotron emission.

In conclusion, the method described in this article must be considered an attempt at developing techniques for the global visualization of turbulent and coherent structures with microwave reflectometry. Undoubtedly, its practical implementation presents serious difficulties, such as the need for large machine ports and 2D arrays of microwave detectors. Nevertheless, this technique has the potential for providing new and important information on the spatial structure of turbulent fluctuations in tokamaks and spherical tori.

ACKNOWLEDGMENTS

This work was supported by U.S. DOE Contract No. DE-AC02-76-CHO-3073, and by NOW and EURATOM under the EURATOM-FOM association agreement.

[1] W. Horton, Rev. Mod. Phys. **71**, 735 (1999).
[2] J. W. Connor and H. R. Wilson, Plasma Phys. Controlled Fusion **36**, 719 (1994).
[3] ITER Physics Expert Groups on Confinement and Transport, Nucl. Fusion **39**, 2175 (1999).
[4] E. Mazzucato, Phys. Rev. Lett. **36**, 792 (1976).
[5] C. M. Surko and R. E. Slusher, Phys. Rev. Lett. **37**, 1747 (1976).
[6] D. L. Brower, W. A. Peebles, and N. C. Luhmann, Jr., Nucl. Fusion **27**, 2055 (1987).
[7] R. Philipona, E. J. Doyle, N. C. Luhmann, Jr. *et al.*, Rev. Sci. Instrum. **61**, 3007 (1990).
[8] P. Devynck, X. Garbet, C. Laviron *et al.*, Plasma Phys. Controlled Fusion **35**, 63 (1993).
[9] R. Fonck, G. Cosby, R. D. Durst *et al.*, Phys. Rev. Lett. **70**, 3736 (1993).
[10] E. Mazzucato and R. Nazikian, Phys. Rev. Lett. **71**, 1840 (1993).
[11] R. Nazikian and E. Mazzucato, Rev. Sci. Instrum. **66**, 392 (1995).
[12] E. Mazzucato, Rev. Sci. Instrum. **69**, 2201 (1998).
[13] E. Mazzucato, Nucl. Fusion **41**, 203 (2001).
[14] S. O. Rice, Bell Syst. Tech. J. **23**, 282 (1944); **24**, 96 (1945) [reprinted in N. Wax, *Selected Papers on Noise and Stochastic Processes* (Dover, New York, 1954)].
[15] E. Mazzucato, Rev. Sci. Instrum. **69**, 1691 (1998).
[16] P. L. Hsu, B. H. Deng, J. Wang, C. W. Domier, and N. C. Luhmann, Jr., Rev. Sci. Instrum. **72**, 364 (2001).
[17] M. Ono, S. M. Kaye, M. Peng *et al.*, Nucl. Fusion **40**, 557 (2000).
[18] U. Samm, in *Proceedings of the 16th IEEE Symposium on Fusion Engineering, 1995* (IEEE, Piscataway, NJ, 1995), p. 470.
[19] A. J. H. Donné, R. Jaspers, C. J. Barth *et al.*, Rev. Sci. Instrum. **72**, 1046 (2001).
[20] B. H. Deng, C. W. Domier, N. C. Luhmann, Jr. *et al.*, Rev. Sci. Instrum. **72**, 301 (2000).